Journal Name

ARTICLE

Cite this: DOI: 10.1039/x0xx00000x

Organoaluminium complexes of *ortho-*, *meta-*, *para*-anisidines: Synthesis, structural studies and ROP of ε-caprolactone (and *rac*-lactide).

Yuanzhan Li,[a] Ke-Qing Zhao,[a] Mark R.J. Elsegood,[b] Timothy J. Prior,[c] Xinsen Sun,[c] Shanyan Mo[c] and Carl Redshaw[a,c]*

Received 00th January 2014,
Accepted 00th January 2014

DOI: 10.1039/x0xx00000x

Abstract: Reaction of Me_3Al (two equivalents) with *ortho-*, *meta-* or *para*-anisidine, $(OMe)(NH_2)C_6H_4$, affords the complexes $\{[1,2\text{-}(OMe),N\text{-}C_6H_4(\mu\text{-}Me_2Al)](\mu\text{-}Me_2Al)\}_2$ (**1**), $[1,3\text{-}(Me_3AlOMe),NHC_6H_4(\mu\text{-}Me_2Al)]_2$ (**2**) or $[1,4\text{-}(Me_3AlOMe),NHC_6H_4(\mu\text{-}Me_2Al)]_2$ (**3**), respectively. The molecular structures of **1** - **3** have been determined and all three complexes were found to be highly active for the ring opening polymerization (ROP) of ε-caprolactone either with or without benzyl alcohol present; at various temperatures, the activity order **1** > **2** ≈ **3** was observed. For the ROP of *rac*-lactide results for **1** – **3** were poor.

Introduction

The ring opening polymerization (ROP) of cyclic esters to produce biodegradable polymers continues to be an area of immense academic interest. A variety of metal-based initiators have been employed, which operate via a coordination-insertion mechanism. Aluminium complexes too have attracted attention in this area, primarily due to their beneficial toxicity (low) and Lewis acidity (high). [1] Of the previously reported organoaluminium systems, most studies have centred around the use of *N*,*O*-phenoxyimine (salicylaldimine) type ligand sets (see **I**, chart 1). [2] For example, Nomura and co-workers studied the series of dimethylaluminium complexes $[Me_2Al[O\text{-}2\text{-}R^1\text{-}6\text{-}(R^2N{=}CH)C_6H_3]$ (R^1 = Me, *t*Bu; R^2 = *t*Bu, cyclohexyl, adamantyl, Ph, 2,6-$Me_2C_6H_3$, 2,6-*i*$Pr_2C_6H_3$), for which it was found that the imine bound substituent (R^2) had a significant influence on the observed catalytic activity. [2a,d] As well as other systems derived from other bi-dentate chelates, for example the *N*,*N*- *O*,*O*- chelate systems **II** – **IV**, [3] recent studies have also focussed on the use of tri- (eg. **V** and **VI**), [1c, 4] and tetra-dentate ligand sets (eg. **VII** and **VIII**) [5]; macrocyclic ligands have also been studied. [6] These multi-dentate ligands, which are usually derived from amines/anilines, have been shown to yield complexes capable of the ROP of ε-caprolactone in a living manner, allowing for control over the molecular weight and distribution of the resulting polymer product. [3] We have also found that remote dialkylaluminium centres present in the same complex can have beneficial cooperative effects on the catalytic activity as long as they are not linked by aluminoxane type bonding. [6] With this in mind, we are exploring the potential of functionalised anilines as ancillary ligands at aluminium in the ROP of ε-caprolactone or *rac*-lactide, where there is the potential for binding multiple organoaluminium centres in relatively close proximity. Herein, we present our findings on systems derived from the interaction of *o-*, *m-*, *p*-anisidines with trimethylaluminium and explore the effect of the structures of the resulting organoaluminium derived species on catalytic activity in the ROP of ε-caprolactone; activities for the ROP of *rac*-lactide were very and so further studies were discontinued.

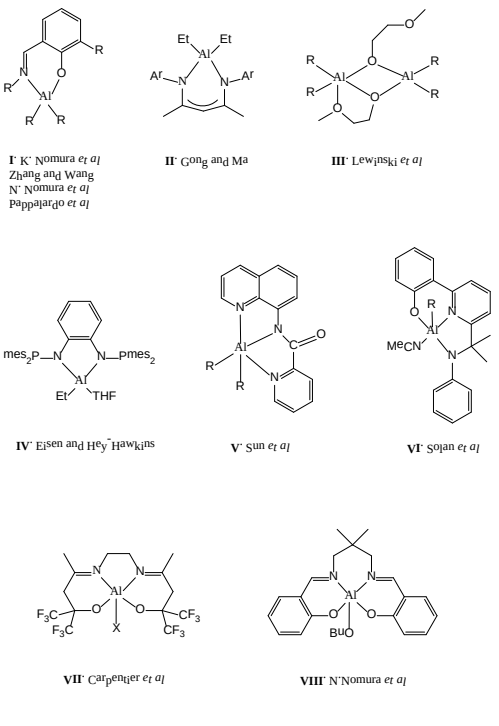

Chart 1· Repor̈ted organoaluminium ROP pre-catalysts

Results and Discussion

Interaction of *o*-anisidine with two equivalents of Me_3Al in toluene afforded the complex {[1,2-(OMe),N-C_6H_4(μ-Me_2Al)](μ-Me_2Al)}$_2$ (**1**) in good isolated yield (~ 77 %). Slow cooling of the reaction to 0 °C led to the formation of colourless crystals suitable for a single crystal X-ray diffraction study. The molecular structure of **1** is shown in Figure 1, with selected bond lengths and angles given in the caption. The centrosymmetric dimer possesses slightly asymmetric Me_2Al bridges, which link the *o*-anisidine-derived fragments via the N centres. Within each *o*-anisidine-derived fragment, a four coordinate pseudo tetrahedral Me_2Al group bridges the OMe and N centres.

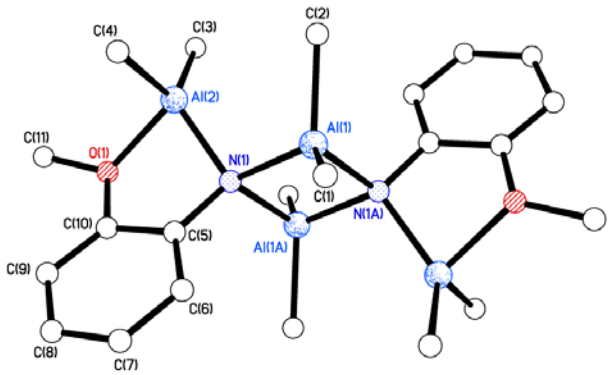

Figure 1. Molecular structure of **1** showing the atom numbering scheme. Selected bond lengths (Å) and angles (°): Al(1) – N(1) 1.9454(11), Al(1) – N(1A) 1.9627(11), Al(2) – N(1) 1.9164(11), Al(2) – O(1) 1.9645(10); N(1) – Al(1) – N(1A) 89.82(4), N(1) – Al(2) – O(1) 84.10(4).

Similar use of *m*-anisidine failed to produce any crystalline product on cooling of a saturated toluene solution, instead it proved necessary to add an equal volume of *n*-hexane and cool the resulting toluene/hexane solution to -78 °C, whereupon a while crystalline product formed, albeit in much lower isolated yield (~ 21 %). Use of solely toluene tended to result in the formation of sticky (off-white) oil, which more often than not would fail to crystallize. The molecular structure of **2** is shown in Figure 2, with selected bond lengths and angles given in the caption. In contrast to complex **1**, the 1,3-deposition of the functional groups in the *m*-anisidine resulted in a centrosymmetric dimer which contains terminal Me_3Al groups bound at the OMe function. The *m*-anisidine-derived fragments are linked via Me_2Al bridges with retention of a NH group.

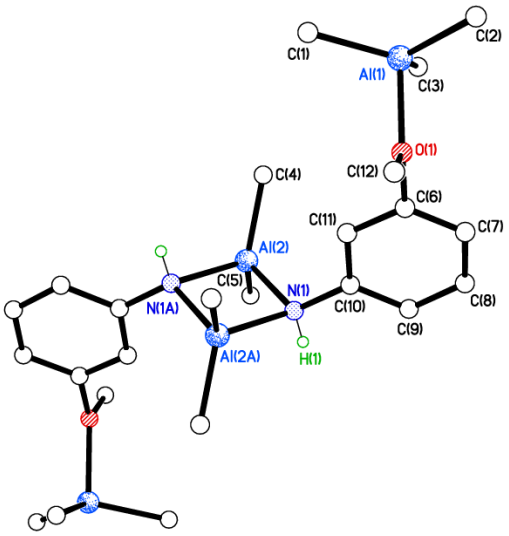

Figure 2. Molecular structure of **2** showing the atom numbering scheme. Selected bond lengths (Å) and angles (°): Al(1) – O(1) 1.9600(13), Al(2) – N(1) 1.9802(15), Al(2) – N(1A) 1.9807(15); Al(1) – O(1) – C(6) 126.35(10), N(1) – Al(2) – N(1A) 87.67(6), Al(2) – N(1) – C(10) 119.57(9).

An analogous product to **2** was obtained when employing *p*-anisidine as starting material, *viz* [*p*-(Me_3AlOMe),NHC_6H_4(μ-Me_2Al)]$_2$ (**3**), which can be readily recrystallized from a saturated toluene solution on prolonged standing at ambient temperature (isolated yield ~ 48 %). The molecular structure of **3** is shown in Figure 3, with selected bond lengths and angles given in the caption. The molecular arrangement of **3** is very similar to that present in **2**; a centrosymmetric dimer is formed from the two *p*-anisidine derived groups and two Me_2Al bridges. The OMe function of each *p*-anisidine is bound to a terminal Me_3Al group.

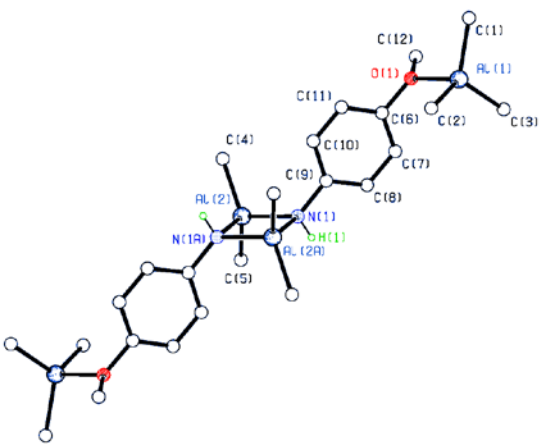

Figure 3 Molecular structure of 3 showing the atom numbering scheme. Selected bond lengths (Å) and angles (o): Al(1) – O(1) 1.9582(19), Al(2) – N(1) 1.9851 (15), Al(2) – N(1A) 1.9809 (15); Al(1) – O(1) – C(6) 120.28(10), N(1) – Al(2) – N(1A) 87.24(6), Al(2) – N(1) – C(10) 120.62(14).

Table 1. Ring Opening Polymerization screening of ε-CL by pre-catalysts **1**.

Entry	Cat.	CL:X[b]:BnOH	*T*/°C	*t*/min	m/g	Yield (%)	M_n*10^{-4}[c]	PDI
1	1	250:01:01	110	30	2.26	82.0	1.84	1.73
2	1	250:01:01	80	30	2.72	98.7	2.04	1.80
3	1	250:01:01	60	30	1.37	49.7	1.41	1.62
4	1	250:01:01	40	30	1.21	43.9	1.37	1.55
5	1	250:01:01	25	30	0.88	31.9	0.96	1.47
6	1	250:01:00	110	30	2.02	73.3	1.65	1.72
7	1	250:01:00	80	30	2.54	92.2	1.98	1.85
8	1	62.5:01:01	80	30	2.08	75.6	0.53	1.88
9	1	125:01:01	80	30	2.16	78.4	0.90	1.98
10	1	500:01:01	80	30	2.56	93.1	2.16	1.88
11	1	1000:01:01	80	30	0.32	11.6	2.74	1.98

[a] Conditions: 20 μmol of cat.; 1.0 M ε-CL toluene solution. [b] X = Al-anisidine complexes [c] GPC data in THF *vs* polystyrene standards.

Ring-Opening Polymerization (ROP) of ε-Caprolactone (ε-CL).

Aluminium compounds are often reported as efficient catalysts for ring-opening polymerization (ROP) of cyclic esters. [1] The catalytic behaviour of **1** - **3** was explored toward the ROP of ε-CL. Generally these complexes exhibited good activity for the ROP of ε–CL. Runs were observed over 30 min, results for which are summarized in Table 1. Moreover, the detailed investigations for the optimization of the conditions were conducted by employing **1** as the initiator, the results for which are collected in Table 1.

The pre-catalyst **1** was effective in the ROP of ε-CL both in the presence and absence of benzyl alcohol (BnOH) (Table 1, entries 1–7) though lower activities was observed in the absence of benzyl alcohol, although such conditions produced polymers with a similar molecular weight distribution. Given that the aluminium complex, in the presence of benzyl alcohol, exhibited better activity, detailed investigations of complex **1–3** have been carried out in the presence of BnOH (Table 1).

According to entries 1–5 in Table 1, a linear relationship between the monomer conversions and M_n values was observed with narrow molecular weight distributions [1.47–1.80], indicating the classical feature of a living polymerization process (Fig. 4). The molecular weight distributions [PDI] values of the resultant polymers became a little broader with increased monomer conversions [e.g., PDI: 1.47 (conversion 31.9 %), 1.41 (conversion 43.9 %), 1.73 (conversion 82.0 %), and 1.80 (conversion 98.7 %) in Table 1].

Table 1 displays result for elevation of the temperature (Table 1, entries 1–5), which resulted in higher molecular weight polymer and a higher conversion rate until 85 °C, and decreased at higher temperatures for **1**.

As high-molecular-weight polyesters possess better mechanical properties for subsequent utilization, high-molecular-weight PCL is an attractive target. An increase of the monomer/Al ratio often leads to higher molecular weights; however, this is usually to the detriment of the monomer conversion rate. Here, we also investigated the effect of the ε-CL/Al molar ratio on the catalytic behaviour, and the results are given in Table 1 (entries 2, and 8–11). When the mole ratio CL: Al was increased from 62.5 to 1000, the molecular weight increased from 0.53×10^4 to 2.74×10^4 with little change of molecular weight distribution (1.88–1.98), but the conversion rate significantly decreased, producing polymers with lower molecular weight than the calculated M_n values (Figure. 5).

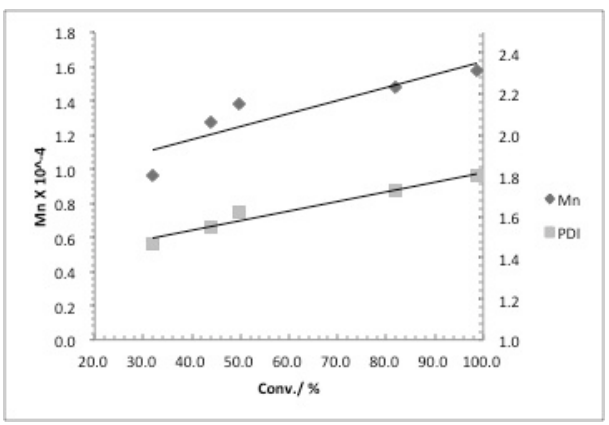

Figure 4. M_n and M_w/M_n *vs*. monomer conversion in the ROP of ε-CL initiated by **1**/ *o*-anisidine aluminium complex (Table 1, entries 1–5).

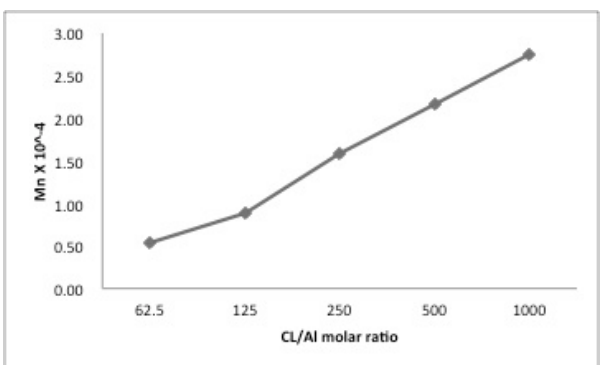

Figure 5. Plots of M_n values *vs*. CL/Al molar ratio in the ROP of ε-CL initiated by **1** (Table 1, entries 2, and 8–11).

Table 2. Ring Opening Polymerization screening of *ε*-CL by pre-catalysts **1** to **3**.[a]

Entry	Cat.	CL:X[b]:BnOH	*T*/◦C	*t*/min	m/g	Yield (%)	M_n*10^{-4} [c]	PDI
1	1	250:01:01	110	30	2.26	82.0	1.84	1.73
2	2	250:01:01	110	30	1.79	64.9	1.16	1.73
3	3	250:01:01	110	30	1.71	62.0	1.02	1.10
4	1	250:01:01	80	30	2.72	98.7	2.04	1.80
5	2	250:01:01	80	30	2.56	92.9	1.06	1.95
6	3	250:01:01	80	30	2.67	96.9	1.16	1.37
7	1	250:01:01	25	30	0.88	31.9	0.96	1.47
8	2	250:01:01	25	30	0.79	28.7	0.70	1.53
9	3	250:01:01	25	30	0.8	29.0	0.69	1.16

[a] Conditions: 20 μmol of cat.; 1.0 M *ε*-CL toluene solution. [b] X = Al-anisidine complexes [c] GPC data in THF *vs* polystyrene standards.

In addition, we investigated the behaviour of the other complexes herein toward the ROP of *ε*-CL. Generally, the anisidine aluminium complexes showed good catalytic activity with high conversion (> 90 %). The activity order **1** > **2** ≈ **3** was observed, with **1** clearly outperforming **2** and **3** at 110 ºC. The effect on the molecular weight of the polymer also exhibited the same order. Despite the similar conversion rates and molecular weights obtained using **2** and **3** at different temperatures (Table 2, entries 2, 3, 5, 6, 8 and 9), the molecular weight distributions using **3** were somewhat smaller, compared with **2** [e.g., PDI: 110 °C (1.73 *vs* 1.10), 85 °C (1.95 *vs* 1.37), and 25 °C (1.53 *vs* 1.16) in Table 2]. This is attributed to the ease with which **3** can be reproducibly crystallized on a large scale.
In order to compare the systems herein with others in the literature, we screened the complexes $Me_2Al[O\text{-}2\text{-}tBu\text{-}6\text{-}(RN{=}CH)C_6H_3]$ (R = *t*Bu, C_6F_5) under the same conditions. [2a,d] For R = C_6F_5, the system exhibited a yield of 94.7 % at 60 ºC over 60 min, whereas for R = *t*Bu, the systems was virtually inactive (yield < 10 %) – see Table S1 (ESI).

Ring-Opening Polymerization (ROP) of *rac* -Lactide (LA).
The ROP of *rac*-Lactide (LA) using **1–3** was conducted both in the presence and absence of BnOH. Disappointingly, these aluminium compounds exhibited very low activity (see Table. 3) and therefore further investigations were discontinued.

Table 3. Ring Opening Polymerization screening of *rac* -LA by pre-catalysts **1** to **3**.[a]

Entry	Cat.	CL:X[b]:BnOH	*T*/◦C	*t*/min	m/g	Yield (%)
1	1	250:01:01	80	30	0.13	4.7
2	3	250:01:01	80	30	0.08	2.9
3	1	250:01:01	110	30	0	0.0
4	3	250:01:01	110	30	0	0.0
5	1	250:01:01	80	24h	0.19	6.9
6	3	250:01:01	80	24h	0.13	4.7
7	1	250:01:00	80	24h	0	0.0
8	3	250:01:00	80	24h	0	0.0

[a] Conditions: 20 μmol of cat.; 1.0 M *ε*-CL toluene solution. [b] X = Al-anisidine complexes

In conclusion, we have treated *o*-, *m*- and *p*-anisidine each with two equivalents of trimethylaluminium. Crystal structure analyses of the products revealed that in the case of the *ortho*-anisidine, a complex containing two types of Me_2Al bridge is formed, namely $\{[1,2\text{-}(OMe),N\text{-}C_6H_4(\mu\text{-}Me_2Al)](\mu\text{-}Me_2Al)\}_2$ (**1**). By contrast, as a result of the increased distance between the methoxy and amino functionalities, both the *meta*- and *para*-anisidines react to form dimeric complexes containing an Me_3Al group bound to each methoxy group, namely $\{[1,3\text{-}(Me_3AlOMe),NH\text{-}C_6H_4](\mu\text{-}Me_2Al)\}_2$ (**2**) and $\{[1,4\text{-}(Me_3AlOMe),NH\text{-}C_6H_4](\mu\text{-}Me_2Al)\}_2$ (**3**), respectively. In terms of the ROP of *ε*-caprolactone, complexes **1 - 3** can efficiently promote the ROP of *ε*-caprolactone both in the presence and absence of BnOH. Complex **1** afforded highest activity, particularly at 110 ºC, and, given the molecular structures, this is tentatively attributed to the close proximity of the two Me_2Al bridging groups in **1**. It is noteworthy that we have previously observed beneficial cooperative effects for two Me_2Al groups positioned 5.7818(10) Å apart in a macrocyclic system; [6] closer Al – Al interactions in such systems (< 3.2270(14) Å) hindered the polymerization process. Herein, the Al(1) ··· Al(2) distance in the best performing system, namely the '*ortho*' complex **1** is 3.394 Å, whereas in the '*meta*' and '*para*' complexes, the distance is somewhat shorter, for example in **2**, the Al(2) – Al(2A) distance is 2.8573(8) Å.

Table 4. Crystallographic data for complexes **1**, **2** and **3**.

Identification code	1	2	3
Chemical formula	C22H38Al4N2O2	C24H46Al4N2O2·C7H8	C24H46Al4N2O2
Formula weight	470.46	594.68	502.55
Temperature K	150(2)	150(2)	150(2)
Radiation MoK □, wave	0.71073	0.71073 Å	0.71073 Å
Crystal system, space group	monoclinic, P21/n	monoclinic, P21/n	triclinic, P-1
a/ Å	8.7510(7)	7.1092(4)	7.3610(9)
b/ Å	15.3173(12)	21.2450(12)	10.0951(12)
c/ Å	10.1026(8)	12.3300(7)	10.6561(14)
α/°	90	90	103.037(10)
β/°	90.133(2)	92.839(2)	95.097(10)
γ/°	90	90	96.205(10)
V/ Å3	1354.17(19)	1859.98(18)	761.67(16)
Z	2	2	1
Calculated density Mg m-3	1.154	1.085	1.096
Absorption coefficient □1 mm	0.19	0.15	0.17
F(000)	504	644	272
Crystal colour	colourless	colourless	colourless
Crystal size	0.61 × 0.30 × 0.09 mm3	0.73 × 0.11 × 0.07	0.36 × 0.19 × 0.17
Reflections for cell refinement	6528	6768	5427
Data collection method	Bruker SMART 1000 CCD Diffractometer □ rotatio with narrow frames	Bruker SMART 1000 CCD Diffractometer □ rotation with narrow frames	Stoe IPDS2 Diffractometer □ rotat with 1° frames.
□ range for data collection	2.4 to 28.8°	2.5 to 28.4°	2.0 to 29.2
Index ranges	h –11 to 11, k –20 to 19, l –13 to 13	h –9 to 9, k –28 to 27, l –15 to 16	h −10 to 8, k −13 to 13, l –14 to 14
Completeness to □ = 26.00°	100.0 %	99.9 %	98.4 %
Intensity decay	0 %	0 %	0 %
Reflections collected	11499	15849	7591
Independent reflections	3228 (Rint = 0.0206)	4408 (Rint = 0.0192)	3999 (Rint = 0.0586)
Reflections with F2>2 □	2703	3453	2412
Absorption correction	semi-empirical from equivalents	semi-empirical from equivalents	face-indexed (Tompa method)
Min. and max. transmission	0.892 and 0.983	0.896 and 0.989	0.9784 and 0.9564
Structure solution	direct methods	direct methods	direct methods
Refinement method	Full-matrix least-squares on F2	Full-matrix least-squares on F2	Full-matrix least-squares on F2
Weighting parameters a, b	0.052, 0.3059	0.0486, 0.7440	0.051, none
Data / restraints / parameters	3228 / 0 / 157	4408 / 52 / 235	3999 / 2/ 154
Final R indices [F2>2 □]	R1 = 0.033, wR2 = 0.097	0.039 0.107	0.041 0.093
R indices (all data)	R1 = 0.0416, wR2 = 0.0977	0.0592 0.1367	0.0780 0.1026
Goodness-of-fit on F2	1.08	1.03	0.859
Largest and mean shift/su	0.001 and 0.000	0.001 and 0.000	0.001 and 0.000
Largest diff. peak and hole/ e Å–3	0.3 and –0.22	0.31 and –0.20	0.351 and −0.254

Experimental

General: All manipulations were carried out under an atmosphere of dry nitrogen using conventional Schlenk and cannula techniques or in a conventional nitrogen-filled glove box. Toluene was refluxed over sodium. Acetonitrile were refluxed over calcium hydride. All solvents were distilled and degassed prior to use. IR spectra (nujol mulls, KBr windows) were recorded on a Nicolet Avatar 360 FT IR spectrometer; ^{1}H NMR spectra were recorded at room temperature on a Varian VXR 400 S spectrometer at 400 MHz or a Gemini 300 NMR spectrometer or a Bruker Advance DPX-300 spectrometer at 300 MHz. The ^{1}H NMR spectra were calibrated against the residual protio impurity of the deuterated solvent. Elemental analyses were performed by the elemental analysis service at the London Metropolitan University and Sichuan Normal University, Chengdu, Sichuan. The anisidine reagents were purchased from Sigma Aldrich and were used as received.

Synthesis of {[1,2-(OMe),N-C_6H_4(μ-Me_2Al)](μ-Me_2Al)}$_2$ **(1)** Me_3Al (16.5 ml, 1.0 M in toluene, 16.5 mmol) was added slowly to *o*-anisidine (0.92 ml, 8.1 mmol) at ambient temperature. The system was then refluxed for 12 h, and allowed to cool to room temperature.On prolonged standing (1 – 2 days), crystals of **1** formed, yield: 1.47 g, 77 %; further crops of crystals can be obtained from the mother liquor on prolonged standing at 0 °C. $C_{22}H_{38}Al_4N_2O_2$ Calcd: C 56.2, H 8.1, N 6.0. Found: C 55.9, H 8.0, N, 6.1 % IR: 1599w, 1574w, 1307w, 1277m, 1218s, 1198s, 1156s, 1109s, 1036w, 1006s, 921w, 854s, 772m, 756m, 722s, 647m. Mass spec (EI, positive mode): 471 M^+, 456 M^+ - CH_3, 426 M^+ - 2CH_3, 399 M^+ - Al$(CH_3)_2$, 384 M^+ - Al$(CH_3)_2$ – CH_3. ^{1}H NMR (400 MHz, C_6D_6, 298 K) δ: 6.98 – 6.80 (overlapping m, 8H, aryl*H*), 3.76, 3.73 (2x s, 6H, O*Me*), -0.98 (s, 12H, Me_2Al). ^{13}C NMR (C_6D_6) δ: 148.97, 148.78, 141.29, 140.68, 124.96, 121.18, 121.08, 110.94, 110.71 (all aryl*C*), 56.8, 56.7 (2x O*Me*), -5.33, -8.85 (2x *Me*$_2$Al).

Synthesis of {[1,3-(Me_3AlOMe),NH-C_6H_4](μ-Me_2Al)}$_2$ **(2)**

As for **1**, but using Me_3Al (16.5 ml, 1.0 M in toluene, 16.5 mmol) and *m*-anisidine (0.92 ml, 8.2 mmol). On cooling, hexane (30 ml) was added to afford **2** as an off-white solid on prolonged cooling at -78 ºC, isolated yield 0.41 g, 21 %. $C_{24}H_{46}Al_4N_2O_2$ (sample dried *in-vacuo* for 12 h) Calcd: C 57.3, H 9.2, N 5.5 %. Found: C 56.3, H 9.2, N 4.8 %. IR: 3394w, 1622w, 1604w, 1496w, 1260s, 1204w, 1158w,1092s, 1019s,862w, 799s,721w, 687w, 451w. Mass spec (solid, positive ASAP: APCI): 446 (MH^+ - $Al(CH_3)_2$ – toluene), 430 (M^+ - $Al(CH_3)_2$ – CH_3), 388 M^+ - $2Al(CH_3)_2$), 374 (M^+ - $Al(CH_3)_3$ – $Al(CH_3)_2$). ^{1}H NMR (C_6D_6, 298 K) δ: 7.13 – 6.27 (overlapping m, 8H, aryl*H*), 3.41, 3.39 (2x s, 6H, O*Me*), 3.27, 3.21 (2x s, 2H, N*H*), -0.39 (s, 18H, Me_3Al), -0.49, 0.50 (2x s, 12H, Me_2Al). ^{13}C NMR (C_6D_6) δ: 130.5, 130.4, 129.1, 128.3, 125.4, 118.7, 114.0, 113.8, 113.0 (9x aryl*C*; others either coincident or hidden by solvent), 62.8 (OMe), -8.0 (Me_3Al), -9.6 (Me_2Al).

Synthesis of {[1,4-(Me_3AlOMe),NH-C_6H_4](μ-Me_2Al)}$_2$ **(3)**
As for **1**, but using but using Me_3Al (16.5 ml, 1.0 M in toluene, 16.5 mmol) and *p*-anisidine (1.00 g, 8.2 mmol), and the resulting residue was extracted into acetonitrile (20 ml) to afford colourless crystals of **3**. MeCN, isolated yield 0.99 g, 48 %. For **3**•MeCN (648.7) Calcd: C 62.9, H 9.0, N 6.5 %. Found: C, 63.0, H 9.0, N 6.9 %. IR: 3259m, 1883w, 1602w, 1506s, 1344m, 1303w, 1257m, 1238s, 1198s, 1153s, 1104m, 1042w, 1014m, 975s, 934w, 860s, 831m, 808m, 765bs, 710bs, 627w. Mass spec (solid, positive ASAP: APCI): 501 (M - H)$^+$, 449 (M – H – $Al(CH_3)_2$), 372 (M – H - $2Al(CH_3)_2$). (C_6D_6, 298 K) δ: 6.53 – 6.32 (3x m, 8H, aryl*H*), 3.15, 3.13 (2x s, 6H, O*Me*), 3.11, 3.07 (2x s, 2H, N*H*), -0.39 (s, 18H, Me_3Al), -0.48, -0.51, -0.52 (3x s, 12H, Me_2Al). ^{13}C NMR: the sample proved to be too insoluble in C_6D_6 to obtain useful spectra; a 12 h acquisition in $CDCl_3$ allowed us to identify δ 63.17 (O*Me*), -8.58 (Me_3Al), -9.67 (Me_2Al).

Ring opening polymerization. Typical polymerization procedures in the presence of one equivalent of benzyl alcohol (Table 4, run 1) are as follows. A toluene solution of **3** (0.010 mmol, 1.0 mL toluene) and BnOH (0.010 mmol) were added into a Schlenk tube in the glove-box at room temperature. The solution was stirred for 2 min, and then ε-caprolactone (2.5 mmol) along with 1.5 mL toluene was added to the solution. The reaction mixture was then placed into an oil bath pre-heated to the required temperature, and the solution was stirred for the prescribed time. The polymerization mixture was then quenched by addition of an excess of glacial acetic acid (0.2 mL) into the solution, and the resultant solution was then poured into methanol (200 mL). The resultant polymer was then collected on filter paper and was dried *in* vacuo.

Crystallography

Crystal data for **1** and **2** were collected on a Bruker SMART 1000 CCD diffractometer using narrow slice 0.3° ω-scans for **1**. Data were corrected for Lp effects and for absorption, based on repeated and symmetry equivalent reflections [7]. Crystal data for **3** were collected on a Stoe IPDS2 diffractometer using 1º ω-scans. A face index correction was applied.
Structures were solved by direct methods and refined by full matrix least squares on F^2 [8,9]. H atoms were included in a riding model except for H(6) in **1**, H(1) in **3**, for which coordinates were freely refined. Hydrogen atom U_{iso} values were constrained to be 120 % of that of the carrier atom except for methyl, ammonium, and hydroxyl-H (150 %). [10]

CCDC 986715, 986716, and 986717 contain the supplementary crystallographic data for this paper. These data can be obtained free of charge via (please use the link below) by e-mailing data_request@ccdc.cam.ac.uk, or by contacting: The Cambridge Crystallographic Data Centre, 12 Union Road, Cambridge.CB2 1EZ,UK. Fax: +44(0)1223-336033. www.ccdc.cam.ac.uk/data_request/cif

Acknowledgements
We thank Sichuan Normal University for funding and the EPSRC National Mass Spectrometry Service Swansea for data.

Notes and references
[a] College of Chemistry and Materials Science, *Sichuan Normal University, Chengdu, 610066, China.*
[b] Chemistry Department, Loughborough University, Loughborough, Leicestershire, LE11 3TU,U.K.
[c] Department of Chemistry, University of Hull, Hull, HU6 7RX, U.K.

† Electronic Supplementary Information (ESI) available: [details of any supplementary information available should be included here]. See DOI: 10.1039/b000000x/

1. (a) C. K. Williams, *Chem. Soc. Rev*., 2007, **36**, 1573. (b) A. Arbaoui and C. Redshaw, *Polymer Chem*., 2010, **1**, 801. (c) W. Alkarekshi, A. P. Armitage, O. Boyron, C. J. Davies, M. Govere, A. Gregory, K. Singh and G. A. Solan, *Organometallics*, 2013, **32**, 249 and references therein. (d) Y. Liu, W.-S. Dong, J.-Y. Liu and Y.-S. Li, *Dalton Trans*., 2014, **43**, 2244.
2. (a) N. Iwasa, M. Fujiki and K. Nomura, *J. Mol. Cat. A, Chem*., 2008, **292**, 67; (b) C. Zhang and Z.-X. Wang, *J. Organomet. Chem*., 2008, **613**, 3151; (c) N. Iwasa, J. Liu and K. Nomura, *Catal. Commun.*, 2008, **9**, 1148; (d) J. Liu, N. Iwasa and K. Nomura, *Dalton Trans.*, 2008, 3978; (e) N. Iwasa, S. Katao, J. Liu, M. Fujiki, Y. Furukawa and K. Nomura, *Organometallics*, 2009, **28**, 2179; (f) N. Nomura, T. Aoyama, R. Ishii and T. Kondo, *Macromolecules*, 2005, **38**, 5363; (g) D. Pappalardo, L. Annunziata and C. Pellecchia, *Macromolecules*, 2009, **42**, 6056. (h) X.-F. Yu and Z.-X. Wang, *Dalton Trans*., 2013, **42**, 3860. (i) T.-L. Huang and C.-T. Chen. *J. Organomet. Chem*., 2013, **725**, 15. (i) A. Meduri, T. Fuoco, M. Lamberti, C. Pellecchia and D. Pappalardo, *Macromolecules*, 2014, **47**, 534.
1. (a) S. Gong and H. Ma, *Dalton Trans*., 2008, 3345. (b) J. Lewiński, P. Horeglad, K. Wójcik and I. Justyniak, *Organometallics*, 2005, **24**, 4588. (c) F. Majoumo-Mbe, E. Smolensky, P. Lönnecke, D. Shpasser, M.S. Eisen and E. Hay-Hawkins, *J. Mol. Cat.*, 2005, **240**, 91.
2. (a) M. Shen, W. Zhang, K. Nomura and W.-H. Sun, *Dalton Trans.* 2009, 9000.
3. (a) A. Amgoune, L. Lavanant, C. M. Thomas, Y. Chi, R. Welter, S. Dagorne and J.-F. Carpentier, *Organometallics*, 2005, **24**, 6279; (b) M. Bouyahyi, E. Grunova, N. Marquet, E. Kirillov, C. M. Thomas, T. Roisnel and J.-F. Carpentier, *Organometallics*, 2008, **27**, 5815; (c) M. Bouyahyi, T. Roisnel and J.-F. Carpentier, *Organometallics*, 2012, **31**, 1458. (d) N. Nomura, A. Akita, R. Ishii and M. Mizuno, *J. Am. Chem. Soc*., 2010, **132**, 1750.
4. A. Arbaoui, C. Redshaw and D.L. Hughes, *Chem. Commun*., 2008, 4717.
5. SMART (2001), SAINT (2001 & 2008), and APEX 2 (2008) software for CCD diffractometers. Bruker AXS Inc., Madison, USA.
6. G.M. Sheldrick, SHELXTL user manual, version 6.10. Bruker AXS Inc., Madison, WI, USA, (2000).
7. G.M. Sheldrick, *Acta Crystallogr*. 2008, **A64**, 112-122.
8. A.L. Spek, *Acta Crystallogr*. 1990, **A46**, C34.